



Design, optimization and critical analysis of graphene based surface plasmon resonance sensor for DNA hybridization

Yagyesh Kumar¹ · Rishi Mishra¹ · Ekta Panwar² · Jaswinder Kaur³ · Ravi Panwar¹ 

Received: 25 May 2019 / Accepted: 30 September 2019 / Published online: 10 October 2019
© Springer Science+Business Media, LLC, part of Springer Nature 2019

Abstract

In this paper, the design, optimization and critical analysis of Surface Plasmon Resonance sensor is presented, which works on angular interrogation method. It comprises of five layers which are “Prism–Copper–Germanium–Graphene–Sensing medium”. The influence of the chemical potential (μ_c) of graphene on the sensor performance has been studied in detail. Thickness of all the layers has been optimized. Remarkable results are achieved for the optimal thickness of copper and germanium layers as 50 nm and 6 nm respectively, while two layers of graphene having μ_c of 0.5 eV are introduced to boost-up the performance. Best results in terms of detection accuracy, sensitivity and quality factor have been achieved that fulfill the necessary requirements for good sensing applications.

Keywords Surface plasmon resonance · Graphene · Plasmons · Chemical potential · Sensitivity

1 Introduction

SPR sensor has attracted great attention in the field of medical diagnosis, food safety and air quality monitoring (Tamersit and Djefal 2016). Generally, SPR sensors have three major components viz. optical system, transducing medium and electronic system. Optical system provides a light wave of the desired wavelength while transducing medium introduces it to the bio-chemical reactants. The electronic system converts the optical signal into the electrical signal using optoelectronic transducers. Kretschmann and Raether (1968) configuration of the sensor working with angular interrogation method is used for detection of Deoxyribo-Nucleic-Acid (DNA) hybridization (Zeng et al. 2014). It has played a keen role in the domain of molecular biology like DNA hybridization.

✉ Ravi Panwar
rpanwar.iitr@gmail.com; rpanwar@iiitdmj.ac.in

¹ Discipline of Electronics and Communication Engineering, Indian Institute of Information Technology, Design and Manufacturing Jabalpur, Jabalpur, India

² Department of Biotechnology, Indian Institute of Technology Roorkee (IIT Roorkee), Roorkee, India

³ Department of Electronics and Communication Engineering, Thapar Institute of Engineering and Technology, Patiala, India

DNA hybridization is a biological event that evaluates the level of dissimilarity between two samples of DNA to obtain the genetic difference between two organisms. The identification of a specific orientation or muted sequence of thymine 'T' and adenine 'A' or cytosine 'C' and guanine 'G', between nucleotide bonds is involved in the DNA hybridization sensing. Surface Plasmons are the oscillation of free electrons at the interface of metal and dielectric having a dielectric constant of opposite sign which are produced when electromagnetic (EM) wave which is Transverse Magnetic (TM) polarized falls on it (Homola et al. 1999). These free electron oscillations lead to the generation of Surface Plasmon Wave (SPW), which is p-polarized EM wave and uses the energy of light to propagate. Angular interrogation based SPR sensor uses the SPW waves generated at the junction of prism and metal to examine the changes in the RI of sensing medium.

The concentration of SPW wave is much more in the dielectric than in the metal (Homola et al. 1999), it is highly susceptible to the changes in the optical properties of sensing medium. SPR angle is an important parameter in the angular interrogation system, this method provides better control on the light beam and is quite easy to implement in small sensors (Ronald 2013). Monochromatic light source has been used, whose wavelength belongs to near-infrared region (NIR). The light of this wavelength insures minimum damage to biomolecules and other effects like optical non-linearity, Kerr effect, birefringence is also less in the NIR region (Rahman et al. 2018). A detailed discussion regarding such conventional SPR sensor has been presented by (Pandey and Sharma 2018). The metal layer was coated on the base of the prism by the sputtering technique (Biednov et al. 2015). Copper provides a very high degree of accuracy as compared to gold and silver, because of the large SPR ratio (a ratio of real over imaginary part of dielectric constant). Gold has been found to have a poor adsorption property while silver is found to be highly sensitive to oxidation (Verma et al. 2015; Fu et al. 2015). But at the same time sensitivity obtained by using copper metal is very less and hence polished germanium semiconductor with high refractive index (RI) has been used to increase the sensitivity of the sensor (Li 1980). Various researchers have reported that use of dielectric increases the light trapping capability due to which number of free electrons participating in oscillations increases (Xu et al. 2013). An increase in the oscillations increases the concentration of SPW waves and therefore sensitivity increases. Dielectrics also have additional features which are beneficial for SPR sensor like low optical dispersion and transparency in the NIR region. Metal or dielectric are not good adsorbers of biomolecules, therefore a binding material is required for proper detection.

Graphene has high affinity for bio-molecules and serves as a good binding agent due to the large surface area (Mishra et al. 2016). The binding of biomolecules on graphene is strong and stable, due to interaction between aromatic rings of graphene's hexagonal cells and carbon rings in biomolecules. It has several other useful properties like high carrier mobility, good flexibility and mechanical strength (Pumera 2011). Recently, various optoelectronic devices like ultra-fast lasers, solar cells and polarizers are also incorporating graphene (Geim and Konstantin 2010; Bonnaccorso et al. 2010; Muller et al. 2010; Xia et al. 2009; Zheng et al. 1992). Various researchers have also reported its use as Frequency Selective Surface (FSS) (Mishra et al. 2018; Mishra et al. 2019). But graphene layer causes damping of SPW due to large negative part of RI (Maharana and Jha 2012). Thus germanium can serve as a good candidate to overcome it due to its high light absorption property. Graphene chemical potential (μ_c) is crucial in deciding the performance of SPR sensor, because it has significant impact on RI of graphene (Bludov et al. 2010; Kim et al. 2016). Further, the impact of μ_c on the charge carriers can be explored (Falkovsky 2008; Chu and Gan 2013).

This paper presents a theoretical and mathematical modeling of copper-germanium based, highly sensitive sensor for DNA hybridization. Germanium layer is sandwiched

between copper and graphene to enhance the performance. This paper is organized as follows: in Sect. 2, a theoretical model of structure is developed which consists of optimized layers of different materials and then mathematical modeling is done. Section 3 discusses about the results obtained and at last conclusion is made in Sect. 4. Necessary references are included at the end of the article.

2 Theoretical modeling of sensor

Schematic layout of all the three proposed device configurations is shown in Fig. 1a–c. Configuration-I comprises of three media which are “Prism–Copper–Sensing medium”. Configuration-II incorporates a germanium layer in between the copper and sensing medium. Further, graphene is included in the configuration-III. The material specifications (RI and thickness)

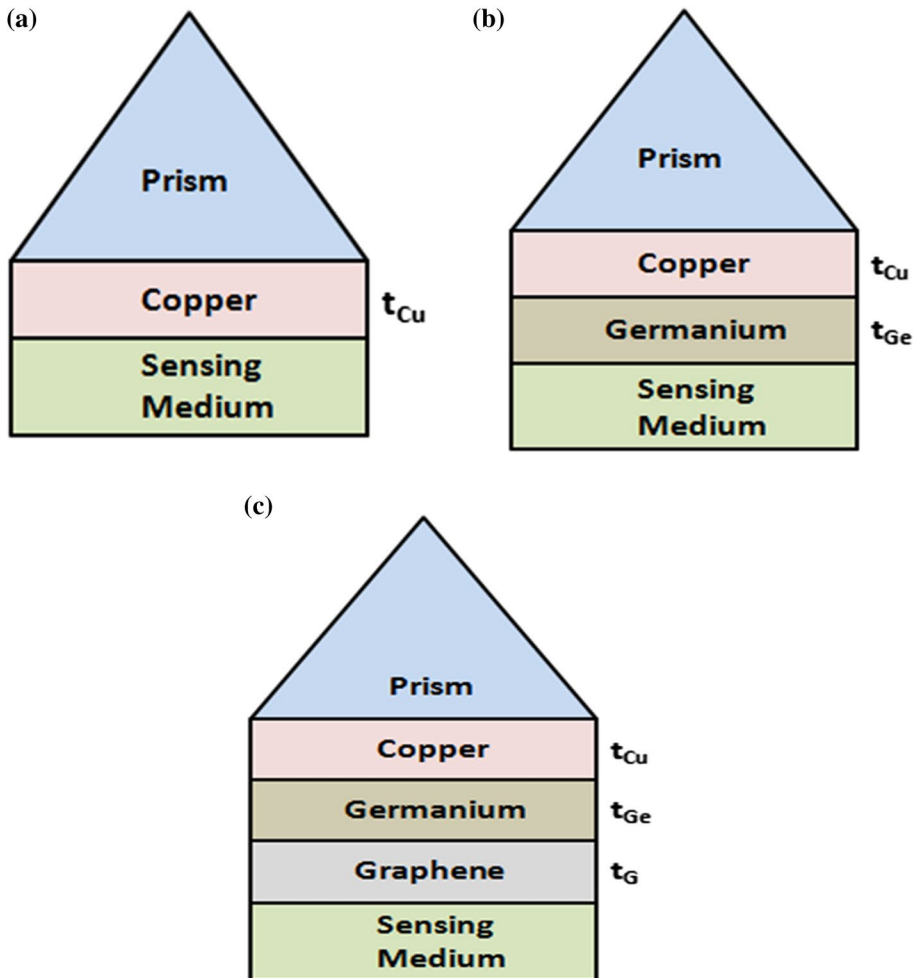


Fig. 1 SPR sensor device configurations **a** configuration-I **b** configuration-II, and **c** configuration-III

are given as follows: prism (SF11) has RI of 1.7786 (Maurya et al. 2015). Copper has RI (n_{Cu}) of $0.01838 + j2.223$ (Mishra et al. 2016) and thickness $d_{Cu} = 50$ nm which has been optimized in the paper. Third is germanium layer, having RI of 5.31 (Li 1980) and optimized thickness (d_{Ge}) of 6 nm. Next is graphene layer having a RI (n_G) of $3 + j1.1487$ and thickness (d_G) of $N \times 0.34$ nm (Verma et al. 2011) where N is the number of layers. At last, fifth layer is sensing medium whose refractive index is considered as 1.33 before the adsorption of molecules. Operating wavelength of light is taken to be 633 nm, which lies in the NIR region.

2.1 Operating principle

The working of SPR sensor can be explained by the angular interrogation method (Ronald 2013). Either monochromatic optical system or sensor which is kept on base is rotated slowly while keeping other one fixed. The intensity of reflected light is monitored continuously. When a particular angle called as resonance angle (θ_{SPR}) is reached, the intensity of reflected light decreases sharply to almost zero. This resonance angle depends on the materials used in the structure, wavelength of light and optical properties of sensing medium. The sudden decrease in intensity of reflected light is due to the formation of Surface Plasmon Waves (SPW) which absorbs the energy from light to propagate. This resonance angle is extremely sensitive to the changes in the concentration of bio-molecules in sensing medium. The change in resonance angle provides very important information to detect DNA hybridization of the sample.

2.2 Mathematical modeling of sensor

Calculation of the reflection intensity has been carried out using N-Layer matrix method (Bao et al. 2011) implemented on the MATLAB platform. According to it the tangential field components of EM wave at first and last boundary are related by Eq. (1) below.

$$\begin{bmatrix} U_1 \\ V_1 \end{bmatrix} = M \begin{bmatrix} U_{n-1} \\ V_{n-1} \end{bmatrix} \tag{1}$$

U_1 and V_1 represents the field at the first boundary, whereas U_{n-1} and V_{n-1} represents the field at the last boundary. The characteristic matrix M of the sensor structure is defined as

$$M_{ij} = \left(\prod_{k=2}^{n-1} M_k \right)_{ij} = \begin{bmatrix} M_{11} & M_{12} \\ M_{21} & M_{22} \end{bmatrix} \tag{2}$$

$$M_k = \begin{bmatrix} \cos \beta_k & (-i \sin \beta_k) / q_k \\ -i q_k \sin \beta_k & \cos \beta_k \end{bmatrix} \tag{3}$$

Where

$$q_k = \left(\frac{\mu_k}{\epsilon_k} \right)^{1/2} \cos \theta_k = \frac{(\epsilon_k - n_1^2 \sin^2 \theta_1)^{1/2}}{\epsilon_k} \tag{4}$$

$$\beta_k = \frac{2\pi}{\lambda} n_k \cos \theta_k (z_k - z_{k-1}) = \frac{2\pi d_k}{\lambda} (\epsilon_k - n_1^2 \sin^2 \theta_1)^{1/2} \tag{5}$$

In the above two equations, d_k denotes the thickness of k th layer, RI and dielectric constant of the k th layer are designated as n_k and ϵ_k . The incident angle of light at first layer is given by θ_1 and wavelength of the light is given by λ . The reflection coefficient of the p-polarized can be written as:

$$r_p = \frac{(M_{11} + M_{12}q_N)q_1 - (M_{21} + M_{22}q_N)}{(M_{11} + M_{12}q_N)q_1 + (M_{21} + M_{22}q_N)} \quad (6)$$

The reflectivity of the device can be expressed as:

$$R_p = |r_p|^2 \quad (7)$$

2.3 Performance evaluation of the sensor

The performance of the SPR sensor has been judged upon sensitivity (S), minimum reflection intensity (R_{\min}), detection accuracy (DA), quality factor (Q), and full width at half maximum (FWHM). All of these terms are quantified as follows:

$$S = \Delta\theta_{res} / \Delta n_s \quad (8)$$

$$DA = \frac{\Delta\theta_{SPR}}{FWHM} \quad (9)$$

$$Q.F = \frac{S}{FWHM(RIU^{-1})} \quad (10)$$

FWHM is the width of the reflectance curve in degrees at the point on the reflectance curve where reflection intensity is half of its maximum value.

2.4 Refractive index and chemical potential of graphene

RI of graphene is highly dependent upon the chemical potential of the graphene. This dependency is expressed by the Kubo formula and the Drude model (Sharma and Dominic 2018), it considers both inter-band and intra-band effect as given below.

$$\sigma_{intra}(\omega) = \frac{je^2\mu}{\pi h^2(\omega + j\tau^{-1})} \quad (11)$$

$$\sigma_{intra}(\omega) = \frac{je^2}{4\pi h} \ln \left(\frac{2|\mu| - (\omega + j\tau^{-1})h}{2|\mu| + (\omega + j\tau^{-1})h} \right) \quad (12)$$

In the above two equations, e is the electronic charge, ω is the angular frequency of the light wave, h is the reduced Planck's constant and τ is the electron relaxation time. RI of graphene is derived from its conductivity by (Bao et al. 2011).

$$\epsilon_{xx} = \epsilon_{yy} = \frac{1 + i\sigma(\omega)}{\omega\epsilon_0 d G_r} \quad (13)$$

where dG_r is the thickness of graphene layer, ϵ_0 is the free space permittivity, σ is the conductivity of graphene, n is the complex RI and ϵ is the dielectric constant.

3 Results and discussions

The basic principle behind the optical wave absorption is the generation of the surface plasmon wave (SPW), which is highly sensitive to the dielectric constant of the material (Homola et al. 1999). It has been observed that the generation of SPW maximizes, when the surface formed by two different kinds of materials have real and complex dielectric constants (DC), respectively (Homola et al. 1999). This phenomenon has been kept in consideration, while designing the SPR-sensor. Moreover, an ideal SPR sensor should have high sensitivity with minimum reflection intensity. It has been observed that the minimum reflection intensity increases with the sensitivity and there is a trade-off between sensitivity and reflection intensity. Hence, the maximum adaptable value (MAV) of reflection intensity has been fixed as 0.1 and maximum sensitivity has been observed in the range of 0.0–0.1 of reflection intensity only.

First, a simple structure (configuration-I), as shown in Fig. 1a, has been considered. The configuration comprises of a prism with real DC, and a thin copper layer (in order of nm) with complex DC, which has two surfaces to produce SPW wave. Figure 2a–c depicts the performance of the proposed configuration. Figure 2a shows the

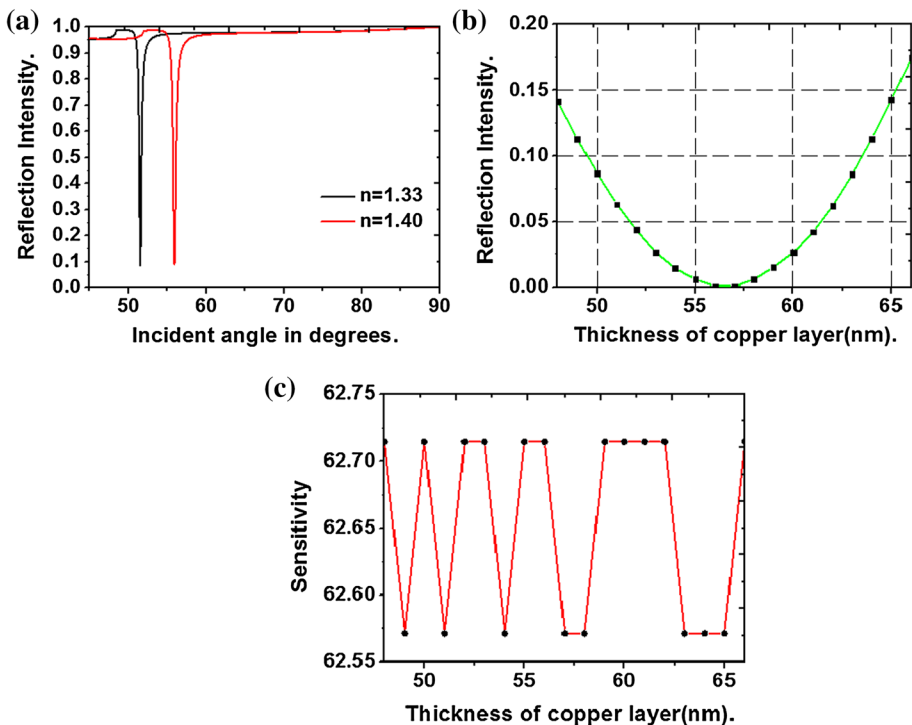


Fig. 2 Performance of configuration-I: **a** reflection intensity v/s incident angle **b** variation in minimum reflection intensity v/s copper layer thickness **(b)** variation in sensitivity v/s copper layer thickness

variation of reflection intensity with angle of incidence for two RI values (i.e., $n = 1.33$ and $n = 1.40$), where Fig. 2b, c presents the variation of reflection intensity and sensitivity over the thickness of the copper layer (t_{cu}), respectively. It can be observed that the sensitivity has zig-zag variation between two values (62.57 and 62.72 approx) with the increment of t_{cu} . While the reflection intensity first decreases and becomes zero at $t_{cu} = 53$ nm and then increases with a further increment of t_{cu} . After considering a trade-off between the reflection intensity and sensitivity and applying the design rule, a sensitivity of 62.71 deg/RIU has been achieved with a minimum reflection intensity of 0.0865. Quite good results have been achieved, but it cannot fulfil the requirements and still there is a possibility to enhance the performance of the device. Hence, in this way, a dielectric layer has been introduced, and the sensitivity and reflection intensity of the device have been analyzed by varying its DC value in the range of 1-6 (i.e., RI from 1 to 6) as depicted in Fig. 3a, b, respectively. The sensitivity increases up to RI=5.6 and then decreases while the reflection intensity remains below the MAV for the entire range of RI. It can be noticed that the maximum absorption has been achieved at a RI value of 5.6, which is close to the RI of germanium, hence it has been considered as a newly inserted dielectric layer. Figure 4a figures the incidence angle dependent reflection intensity of the device (configuration-II). The sensitivity, and reflection intensity spectra's of the configuration-II over the newly inserted germanium layer thickness (t_{Ge}) are shown in Fig. 4 b, c, respectively. It is found that the sensitivity increases with an increment of t_{Ge} , but after 6 nm the reflection intensity exceeds the MAV. Hence, t_{Ge} is restricted to 6 nm, which results 132.00 deg/RIU of sensitivity with minimum reflection intensity of 0.0925 after optimizing all the design parameters.

Since, the DC criteria of the SPW generation have not fulfilled at all the surfaces, there is a chance to further enhance the performance of the device. Hence, a graphene layer (having complex DC value) has been incorporated just after the germanium layer. Graphene is a carbonic material which is bio-friendly and hence, it can be used directly in contact of SM (Sensing Medium). As graphene has a complex DC value, it can fulfil the DC-criteria of the SPW generation. Now, the configuration (configuration-III) has four SPW generating surfaces, which are able to dramatically enhance the device performance. These surfaces are: prism-copper surface, copper-germanium surface, germanium-graphene surface, and graphene-SM surface, as figured in Fig. 1c. An excellent performance has been achieved with this configuration. After optimizing all design parameters, a sensitivity of 160.71 deg./RIU has been achieved with the minimum

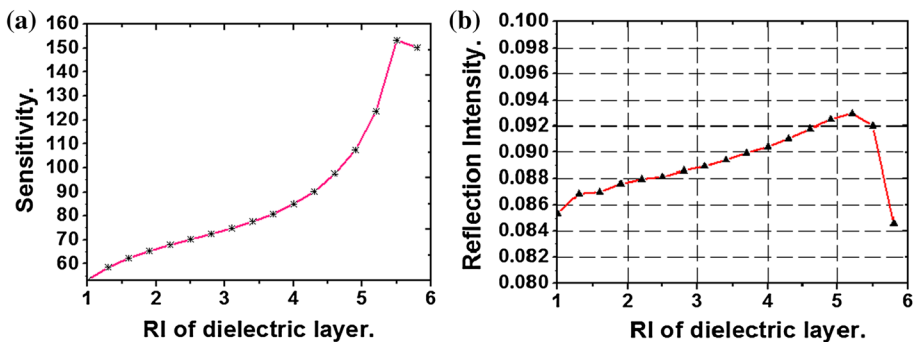


Fig. 3 Effect of refractive index of dielectric layer on **a** sensitivity and **b** reflection intensity of sensor

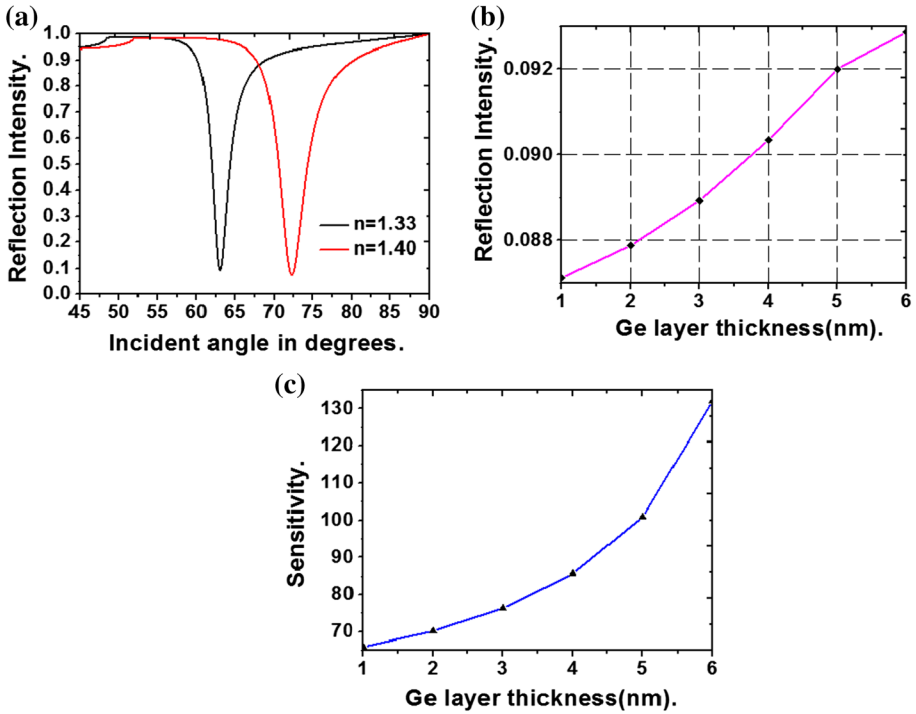


Fig. 4 Performance of configuration II **a** reflection intensity versus incident angle, **b** reflection intensity versus Ge layer thickness, and **c** sensitivity versus Ge layer thickness

reflection intensity of 0.0615. The results are well presented in Fig. 5. Table 1 provides a better comparison of all the configurations carried out in the research work.

Graphene has some unique electrical and optical properties like other carbon-based structures (Knapek et al. 2017), which varies with its layer thickness and μ_c (Mishra et al. 2018; Mishra et al. 2019). Hence, a critical analysis of these parameters has been carried out to analyze the behavior of the graphene layer. Figure 6 a, b depicts the variation of sensitivity, and reflection intensity with an increase in the number of graphene layers, respectively. It can be observed that both sensitivity and reflection intensity increases linearly

Fig. 5 Performance of configuration III: reflection intensity versus incident angle

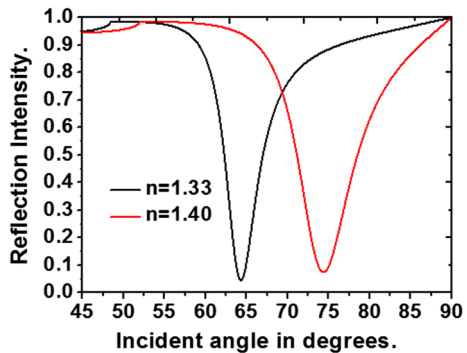


Table 1 Performance parameters of each configuration

Structure	Sensitivity	FWHM	R_{min}	DA	QF
Configuration-I	62.71	0.3	0.0865	14.63	209.04
Configuration-II	132.00	2.39	0.09	3.86	55.23
Configuration-III	160.71	4.95	0.0615	2.27	32.46

with an increment of graphene-layer (from 1 to 3). After two graphene layers, the reflection intensity exceeds MAV, which is not desirable. Hence, the corresponding optimal number of layers can be concluded as 2. Further, the effect of μ_c on the performance of SPR sensor has been explored.

Figure 7 depicts the variation of refractive index of the graphene layer with its chemical potential. It can be observed that real part of refractive index increases from 3 to 4.5, when μ_c varies from 0.2 to 0.4, and then sharply tends to zero at 0.5 eV and then stays almost constant on a further increase in μ_c , whereas the imaginary part follows an opposite trend. It decreases from 2.8 to nearly about 0.1 with increase of μ_c from 0.1 to 0.42 eV and then increases rapidly to 4.5 at 1 eV. Further, the effect of chemical potential on the sensitivity and reflection intensity has been studied by drawing a curve between them as shown in Fig. 8a, b, respectively.

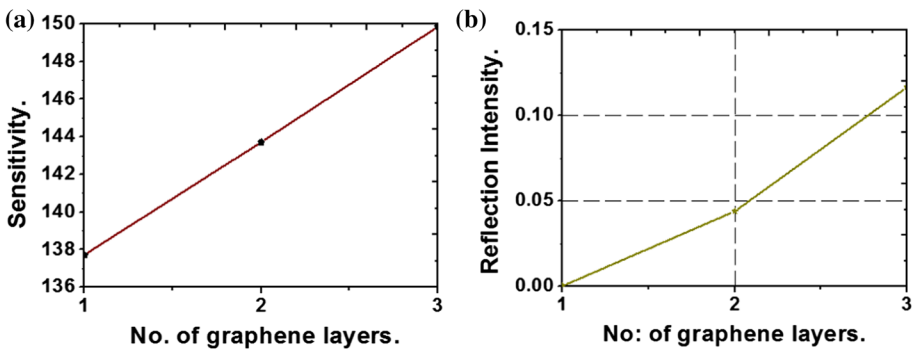
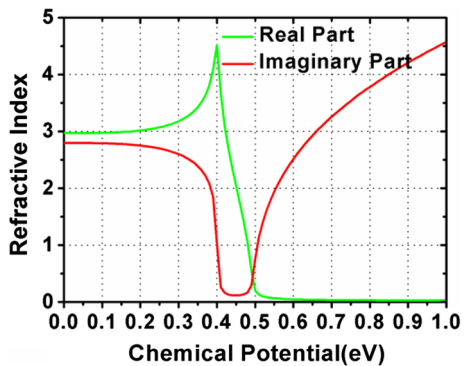


Fig. 6 Plots of sensitivity versus number of graphene layer and minimum reflection intensity versus number of graphene layer

Fig. 7 Refractive index versus chemical potential (eV) of graphene layer



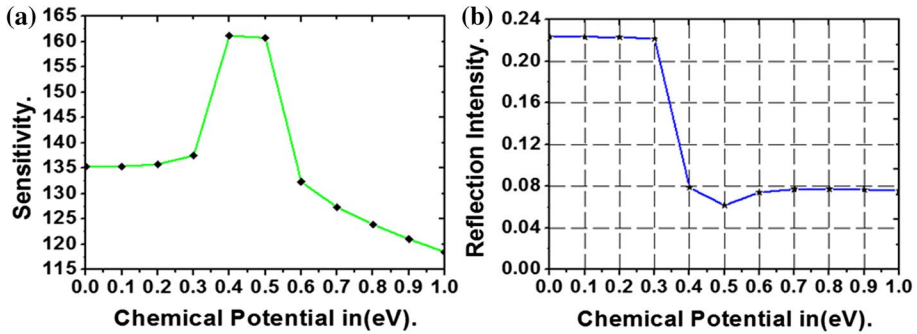


Fig. 8 Effect of graphene chemical potential: **a** sensitivity (deg/RIU) versus chemical potential ‘ μ_c ’ (eV), **b** Minimum reflectance versus chemical potential ‘ μ_c ’ (eV)

It is observed that sensitivity first increases, then remains constant for a small period and then rapidly decreases with peak sensitivity of 149.57 at 0.4 eV, while the value of minimum reflectance follows decreasing staircase type of trend and is greater than 0.1 for a chemical potential of less than 0.5 eV. It is because of the decrease in imaginary RI value of graphene, which can be observed in Fig. 7, and when RI of the graphene becomes pure imaginary, the reflection intensity saturates at 0.08, but the sensitivity goes down simultaneously. Thus, from both the above successive figures, it can be concluded that the optimum result is obtained for μ_c at 0.5 eV. All optimized design variables are well presented in Table 2.

4 Conclusions

In the progressive designing and analysis presented, a highly sensitive and accurate SPR sensor using germanium and copper layer has been developed with minimum possible thickness. An increase in the detection accuracy, sensitivity, and quality factor has been obtained as 100.48%, 165.94% and 166.02% more than conventional sensor, respectively. Further, it has been found that the chemical potential of graphene has significant impact on the sensitivity of the sensor. SPR sensor proposed here can be used for DNA hybridization with better sensitivity and accuracy.

Table 2 Optimal design parameters of each configuration

Design parameter	Configuration-I	Configuration -II	Configuration -III
t_{Cu}	50 nm	50 nm	50 nm
n_{Cu}	0.01838 + j2.223	0.01838 + j2.223	0.01838 + j2.223
t_{Ge}	–	6 nm	6 nm
n_{Ge}	–	5.31	5.31
t_G	–	–	2 × 0.34 nm
n_G	–	–	3 + j1.1487
μ_c	–	–	0.5 eV

Funding Dr. Ravi Panwar would like to acknowledge the Faculty Initiation Grant (FIG) provided by the Indian Institute of Information Technology, Design and Manufacturing to support this work.

References

- Bao, Q., et al.: Broadband graphene polarizer. *Nat. Photonics* **5**(7), 411–415 (2011). <https://doi.org/10.1038/NPHOTON.2011.102>
- Biednov, M., Lebyedeva, T., Shpylovyi, P.: Gold and aluminum based surface plasmon resonance biosensors: sensitivity enhancement. *Optical Sens.* **9506**, 95061P (2015). <https://doi.org/10.1117/12.2177992>
- Bludov, Y.V., Vasilevskiy, M.I., Peres, N.M.R.: Mechanism for graphene-based optoelectronic switches by tuning surface plasmon polaritons in monolayer graphene. *EPL Europhys. Lett.* **92**(6), 161–166 (2010). <https://doi.org/10.1209/0295-5075/92/68001>
- Bonnaccorso, F., Sun, Z., Hasan, T., Ferrari, A.C.: Graphene photonics and optoelectronics. *Nat. Photonics* **4**(9), 611–622 (2010). <https://doi.org/10.1038/nphoton.2010.186>
- Chu, H.S., Gan, C.H.: Active plasmonmic switching at mid-infrared wavelengths with graphene ribbon arrays. *Appl. Phys. Lett.* **102**(23), 231107 (2013). <https://doi.org/10.1063/1.4810003>
- Falkovsky, L.A.: Optical properties of graphene. *J. Phys. Conf. Ser.* **120**(1), 012004 (2008). <https://doi.org/10.1063/1.3525940>
- Fu, H., Zhang, S., Chen, H., Weng, J.: Graphene enhances the sensitivity of fiber optic surface plasmon resonance biosensor. *IEEE Sens. J.* **15**(10), 5478–5482 (2015). <https://doi.org/10.1109/JSEN.2015.2442276>
- Geim, A.K., Konstantin, S.N.: The rise of graphene. In: Rodgers, P. (ed.) *Nanoscience and Technology: A Collection of Reviews from Nature Journals*, pp. 11–19. World Scientific, Singapore (2010). https://doi.org/10.1142/9789814287005_0002
- Homola, J., Yee, S.S., Gauglitz, G.: Surface plasmon resonance sensors. *Sens. Actuators B Chem.* **54**, 3–15 (1999). [https://doi.org/10.1016/S0925-4005\(98\)00321-9](https://doi.org/10.1016/S0925-4005(98)00321-9)
- Kim, S.J., et al.: Characterization of chemical doping of graphene by in situ Raman spectroscopy. *Appl. Phys. Lett.* **108**(20), 203111 (2016). <https://doi.org/10.1063/1.4950969>
- Knapke, A., Sobola, D., Tománek, P., Pokorna, Z., Urbánek, M.: Field emission from the surface of highly ordered pyrolytic graphite. *Appl. Surf. Sci.* **395**, 157–161 (2017). <https://doi.org/10.1016/j.apsusc.2016>
- Kretschmann, E., Raether, H.: Radiative decay of non radiative surface plasmons excited by light. *Zeitschrift für Naturforschung A* **23**(12), 2135–2136 (1968). <https://doi.org/10.1515/zna-1968-1247>
- Li, H.H.: Refractive index of silicon and germanium and its wavelength and temperature derivatives. *J. Phys. Chem. Ref. Data* **9**(3), 561–658 (1980). <https://doi.org/10.1063/1.555624>
- Maharana, P.K., Jha, R.: Chalcogenide prism and graphene multilayer based surface plasmon resonance affinity biosensor for high performance. *Sens. Actuators, B* **169**, 161–166 (2012). <https://doi.org/10.1016/j.snb.2012.04.051>
- Maurya, J.B., Prajapati, Y.K., Singh, V., Saini, S.P.: Sensitivity enhancement of surface plasmon resonance sensor based on graphene—MoS₂ hybrid structure with TiO₂-SiO₂ composite layer. *Appl. Phys.* (2015). <https://doi.org/10.1007/s00339-015-9442-3>
- Mishra, A.K., Mishra, S.K., Verma, R.K.: Graphene and beyond graphene MoS₂: a new window in surface-plasmon-resonance-based fiber optic sensing. *J. Phys. Chem. C* **120**(5), 2893–2900 (2016a). <https://doi.org/10.1021/acs.jpcc.5b08955>
- Mishra, A.K., Mishra, S.K., Verma, R.K.: Graphene and Beyond graphene MoS₂: a window in surface-plasmon-resonance-based fiber optic sensing. *The Journal of Physical Chemistry.* **120**(5), 12 (2016b). <https://doi.org/10.1021/acs.jpcc.5b08955>
- Mishra, R., Panwar, R., Singh, D.: Equivalent circuit model for the design of frequency-selective, terahertz-band, graphene-based metamaterial absorbers. *IEEE Magn. Lett.* **9**, 1–5 (2018). <https://doi.org/10.1109/LMAG.2018.2878946>
- Mishra, R., Sahu, A., Panwar, R.: Cascaded graphene frequency selective surface integrated tunable broadband terahertz metamaterial absorber. *IEEE Photonics J.* **11**(2), 1–10 (2019).. <https://doi.org/10.1109/jphot.2019.2900402>
- Muller, T., Xia, F., Avouris, P.: Graphene photodetectors for high speed optical communications. *Nat. Photonics* **4**(5), 297–301 (2010). <https://doi.org/10.1109/JPROC.2013.2250892>
- Pandey, A.K., Sharma, A.K.: Simulation and analysis of plasmonic sensor in NIR with fluoride glass and graphene layer. *Photonics Nanostructures Fundam. Appl.* **28**, 94–99 (2018). <https://doi.org/10.1016/j.photonics.2017.12.003>

- Pumera, M.: Graphene in biosensing. *Mater. Today* **14**(7–8), 308–315 (2011). [https://doi.org/10.1016/S1369-7021\(11\)70160-2](https://doi.org/10.1016/S1369-7021(11)70160-2)
- Rahman, M.S., Hasan, M.R., Rikta, K.A., Anower, M.S.: A novel graphene coated surface plasmon resonance biosensor with tungsten disulfide (WS₂) for sensing DNA hybridization. *Optical Mater.* **75**, 567–573 (2018). <https://doi.org/10.1016/j.optmat.2017.11.013>
- Ronald Jr., L.E: Multiwavelength Surface Plasmon Resonance Sensor Designs for Chemical and Biochemical Detection. Ph. D thesis, Dept. of Chemistry, Virginia Polytechnic Institute and State University, Ontario, Canada, (2013)
- Sharma, A.K., Dominic, A.: Influence of chemical potential on graphene-based SPR sensor's performance. *IEEE Photonics Technol. Lett.* (2018). <https://doi.org/10.1109/LPT.2017.2776945>
- Tamersit, K., Djeflal, F.: Double-gate graphene nanoribbon field effect transistor for DNA and gas sensing applications: simulation study and sensitivity analysis. *IEEE Sens. J.* **16**(11), 4180–4191 (2016). <https://doi.org/10.1109/JSEN.2016.2550492>
- Verma, R., Gupta, B.D., Jha, R.: Sensitivity enhancement of a surface plasmon resonance based biomolecules sensor using graphene and silicon layers. *Sens. Actuators, B* **160**(1), 623–631 (2011). <https://doi.org/10.1016/j.snb.2011.08.039>
- Verma, A., Prakash, A., Tripathi, R.: Sensitivity enhancement of surface plasmon resonance biosensor using graphene and air gap. *Optics Commun.* **357**, 106–112 (2015). <https://doi.org/10.1016/j.optcom.2015.08.076>
- Xia, F., Muller, T., Lin, Y.M., Sun, F.B.Z., Hasan, T., Ferrari, A.C.: Ultra fast graphene photodetector. *Nat. Nanotechnol.* **4**(12), 839–843 (2009). <https://doi.org/10.1038/nnano.2009.292>
- Xu, J., Xiao, X., Stepanov, A.L., Ren, F., Wu, W., Cai, G., Zhang, S., Dai, Z., Jiang, C.: Efficiency enhancements in Ag nanoparticles-SiO₂-TiO₂ sandwiched structure via plasmonic effect enhanced light capturing. *Nanoscale Res Lett.* **8** **73**(1), 73 (2013). <https://doi.org/10.1186/1556-276X-8-73>
- Zeng, S., Baillargeat, D., Ho, H.P., Yong, K.T.: Nanomaterials enhanced surface plasmon resonance for biological and chemical sensing applications. *Chem. Soc. Rev.* **43**(10), 3426–3452 (2014). <https://doi.org/10.1039/c3cs60479a>
- Zheng, J.P., Jiao, K.L., Shen, W.P., Anderson, W.A., Kwok, Sing, H.: Highly sensitive photodetector using porous silicon. *Appl. Phys. Lett.* **61**(4), 459–461 (1992). <https://doi.org/10.1063/1.107884>

Publisher's Note Springer Nature remains neutral with regard to jurisdictional claims in published maps and institutional affiliations.